EBioMedicine 44 (2019) 554–562

Contents lists available at ScienceDirect

EBioMedicine

journal homepage: www.ebiomedicine.com

EBioMedicine
Published by THE LANCET

Research paper

Impact of acute intraocular pressure elevation on the visual acuity of non-human primates

Mengwei Li [a,1], Nini Yuan [a,1], Xiaoxiao Chen [a], Yiliang Lu [b], Hongliang Gong [b,d], Liling Qian [b], Jihong Wu [a,c,e], Shenghai Zhang [a,c,e], Stewart Shipp [b], Ian Max Andolina [b], Xinghuai Sun [a,c,e,*], Wei Wang [b,d,f,**]

[a] Department of Ophthalmology and Visual Science, Eye, Ear, Nose and Throat Hospital, Shanghai Medical College of Fudan University, Shanghai, China
[b] Institute of Neuroscience, The Center of Excellence in Brain and Intelligence Technology, State Key Laboratory of Neuroscience, Key Laboratory of Primate Neurobiology, Chinese Academy of Sciences, Shanghai, China
[c] State Key Laboratory of Medical Neurobiology, Institutes of Brain Science and Collaborative Innovation Center for Brain Science, Fudan University, Shanghai, China
[d] School of Future Technology, University of Chinese Academy of Sciences, Beijing, China
[e] NHC/Chinese Academy of Medical Sciences Key Laboratory of Myopia (Fudan University), and Shanghai Key Laboratory of Visual Impairment and Restoration (Fudan University), Shanghai, China
[f] Shanghai Center for Brain and Brain-Inspired Intelligence Technology, Shanghai, China

ARTICLE INFO

Article history:
Received 27 March 2019
Received in revised form 18 May 2019
Accepted 28 May 2019
Available online 6 June 2019

Keywords:
Visual acuity
Acute intraocular pressure
Spatial frequency
Optical imaging
Non-human primate

ABSTRACT

Background: Glaucoma is the leading cause of irreversible blindness worldwide and elevated intraocular pressure (IOP) is an established risk factor. Visual acuity, the capacity for fine analysis of spatial frequency (SF) information, is relatively preserved in central vision until the later stages of chronic glaucoma. However, for acute glaucoma that is associated with sharp IOP elevation, how visual acuity is affected by acute IOP elevation remains unclear.
Methods: Using intrinsic-signal optical imaging of large areas of visual cortices V1 and V2 in seven rhesus macaques, visual acuity was directly examined during acute IOP elevation at 70 mmHg, a pressure often observed in acute angle-closure glaucoma. Acute IOP elevation was achieved by reversible monocular anterior chamber perfusions, and visual acuity was quantified by cortical population responses to various SFs ranging from 0.5–6 cycles/°.
Findings: Acute IOP elevation particularly depressed the ability of the visual cortex to register fine details (at high SFs referring to visual acuity), an effect that was progressively more severe toward the central visual field. These results completely contrast with long-term impairments present in chronic glaucoma.
Interpretation: Our results show that impairment of fine visual discrimination within the central visual field is the principal consequence of sharp IOP elevation, implicating relatively greater dysfunction in parvocellular pathways. This study provides direct cortical neural evidence for the immediate visual acuity impairment in acute glaucoma patients.
Fund: National Natural Science Foundation of China, Chinese Academy of Sciences, Shanghai Committee of Science and Technology, and Shanghai Municipal Health Commission.

1. Introduction

Glaucoma, a neurodegenerative disease that involves brain changes, is the leading cause of irreversible blindness worldwide [1]. Higher intraocular pressure (IOP) is an established risk factor associated with the development and progression of glaucoma [2,3]. With elevated IOP, the optic nerve and its visual pathway will be impaired, causing characteristic optic nerve atrophy and visual field defects. According to the degree of IOP elevation, there exist both acute and chronic forms along the glaucoma disease spectrum. For chronic glaucoma, central vision with high acuity is relatively preserved until the later stages of the disease [1]. However, acute angle-closure glaucoma, which is an ophthalmic emergency, can cause sharp IOP elevation (even over 70 mmHg) and might result in visual acuity loss within a short time if there is a delay in treatment [4–6]. Unlike chronic glaucoma, the exact relationship between acute glaucoma and visual acuity is hard to establish because visual acuity is often affected by other factors such as

* Correspondence to: X. Sun, Department of Ophthalmology and Visual Science, Eye, Ear, Nose and Throat Hospital, Shanghai Medical College of Fudan University, 83 Fenyang Road, Shanghai 200031, China.
** Correspondence to: W. Wang, Institute of Neuroscience, The Center of Excellence in Brain and Intelligence Technology, State Key Laboratory of Neuroscience, Key Laboratory of Primate Neurobiology, Chinese Academy of Sciences, 320 Yueyang Road, Shanghai 200031, China.
E-mail addresses: xhsun@shmu.edu.cn (X. Sun), w.wang@ion.ac.cn (W. Wang).
[1] These authors contributed equally to the work.

https://doi.org/10.1016/j.ebiom.2019.05.059

Research in context

Evidence before this study

Many previous clinical studies in chronic glaucoma report that fine visual acuity within the central visual field is relatively preserved until the later stages of the disease. However, for patients with acute glaucoma, because of the high incidence of optical complications such as corneal edema and cataract, the exact relationship between acute IOP elevation and visual acuity is hard to establish clinically. To our knowledge there is no study using non-human primates directly examining the impact of high IOP elevation on the cortical neural population responses and its implications to glaucoma patients, particularly its impact on the neural basis of visual acuity.

Added value of this study

Glaucoma is the leading cause of irreversible blindness. While vision initiates at the retina, it is within the cerebral cortex that seeing ultimately occurs. By using the best experimental model of human vision (non-human old-world primates), we study this important clinical question through optical imaging the visual cortex while reversibly elevating acute IOP to 70 mmHg; a pressure analogous to an acute attack of primary angle-closure glaucoma in humans. Population optical recording across multiple cortical visual areas allows us to assess the biological effects of IOP elevation on visual acuity. We found that acute IOP elevation particularly depressed the ability of the visual cortex to register fine detail, an effect that was progressively more severe toward central visual field. Our work provides direct cortical neural evidence highlighting the immediate visual acuity impairment in acute glaucoma patients.

Implications of all the available evidence

This study in non-human primates identifies cortical deficits indicative of visual acuity loss in acute glaucoma patients. Moreover, considering observations from previous studies focused on chronic glaucoma, this impairment of central visual acuity in an acute non-human primate model implies selective impairment of the parvocellular afferent visual pathway, in distinction to chronic glaucoma in which the parvocellular pathway is more resilient.

corneal edema and complicated cataract [7]. Moreover, the duration and extent of IOP elevation are also unpredictable in acute glaucoma patients. In sum, how acute IOP elevation directly affects visual acuity in human patients remains unclear so far.

Good visual acuity is vital for reading fine print, and it sustains many other important visual functions in our daily life. As such, acuity is routinely examined in clinical practice, for instance by use of the well-known Snellen wall chart. Old world non-human primates possess visual acuity in central field on a par with human observers [8,9], that is selectively abolished by lesions of the parvocellular channel [10]. Experimentally, visual acuity is quantifiably expressed by spatial frequency (SF) tuning for sinusoidal gratings, with the optimal SF for driving cortical responses demonstrating an inverse relationship with retinal eccentricity [11]. Behaviorally, SF perception is mediated jointly through two channels with differing spatiotemporal sensitivities: the magnocellular channel has greater contrast sensitivity for lower SFs and higher TFs (temporal frequencies), whilst the parvocelluar channel is more sensitive to higher SFs and lower TFs [12,13]. Thus, visual acuity deficits in differentiating cortical responses of low and high SFs could indicate the extent of impairment of parvocellular and magnocellular channels for glaucoma patients.

To address directly the above clinical question, we created an acute glaucoma macaque monkey model using anterior chamber perfusion to sharply increase IOP. We measured cortical population responses in the parafoveal regions of primary and secondary visual areas (V1 and V2) by taking advantage of the high spatial resolution and large scale of intrinsic-signal optical imaging, examining the effect of acute elevation of IOP – particularly at 70 mmHg, a level that is often observed during the acute attack phase in angle-closure glaucoma. In contrast to clinical observations in chronic glaucoma patients, we found that acute IOP elevation impairs fine visual discrimination in the central visual field in non-human primates. Our results provide direct cortical neural evidence emphasizing the immediate visual acuity impairment in acute glaucoma patients.

2. Materials and methods

2.1. Animal surgical preparation and maintenance

A total of seven rhesus macaques (*Macaca mulatta*, four males and three females, 4–12 years old, weighing 5.9–10.2 kg) were used in this study. All procedures involving primate experiments were approved by the Animal Ethics Committee of the Eye and ENT Hospital of Fudan University (Shanghai, China).

The animals were fully anesthetized and maintained for intrinsic-signal recording as previously described [14–16]. Anesthesia was first induced with ketamine (15 mg/kg, i.m.). After a tracheotomy, all surgical procedures were performed under gaseous anesthesia (isoflurane 1–2% in 2:1 N_2O:O_2). To obtain V1 and V2, craniotomies were performed to expose large areas posterior to lunate sulcus in both sides of the skull. In all seven monkeys, the exposed cortical regions of V1 and V2 in nine hemispheres were at an eccentricity of approximately 4–9°, and those in five hemispheres were only at an eccentricity of about 3–4°. The sizes of exposed cortical regions varied due to the animal variations such as the size of skulls and the location of lunate sulcus. A 30 mm stainless steel chamber was implanted and secured to the skull with dental cement. Specifically, after a durotomy was performed, the chamber was filled with warm silicone oil and strictly sealed with a coverslip. Subsequent anesthesia for optical imaging was established with loading doses of propofol (4–5 mg/kg/h, i.v.). The pupils were dilated with tropicamide-phenylephrine ophthalmic solution (Santen Pharmaceutical Cor., Ltd. Japan). The anesthesia depth was further confirmed by reflex tests. Paralysis was then maintained by vecuronium bromide (0.16 mg/kg/h, i.v.). Animal's vital life signs were monitored continuously with electrocardiogram, pulse oximeter, temperature, and end-tidal CO_2 throughout the experiment. Refractive errors of the eyes were estimated using a slit ophthalmoscope and corrected with a contact lens when necessary. Each monkey was recorded for 4–5 days and was euthanized by overdosed sodium pentobarbital (~200 mg/kg, i.v) at the end of the experiment.

2.2. Acute IOP elevation

Monocular IOP elevation was induced via a 27-gauge cannula placed in the anterior chamber. Through the cannula, a three-way switch was connected to a pressure transducer and a height-adjustable reservoir containing balanced solution (SINQI Pharmaceutical Cor., China) (Fig. 1a). Normal IOP was set about 15–18 mmHg according to the IOP readout immediately after cannulation. To test the effectiveness of IOP elevation on cortical responses, a wide range of IOP elevations were conducted in one eye of the first monkey. Then four standard levels of IOP elevation (30, 50, 70, and 90 mmHg) were selected, and the rest of six monkeys underwent stepwise IOP elevations to quantifiably evaluate the effect of different IOP elevations on cortical responses (Fig. 1b). An IOP of 70 mmHg, which is analogous to the IOP in the acute attack phase of primary angle-closure glaucoma in humans, was chosen to examine the effect of IOP elevation on the cortical responses to different

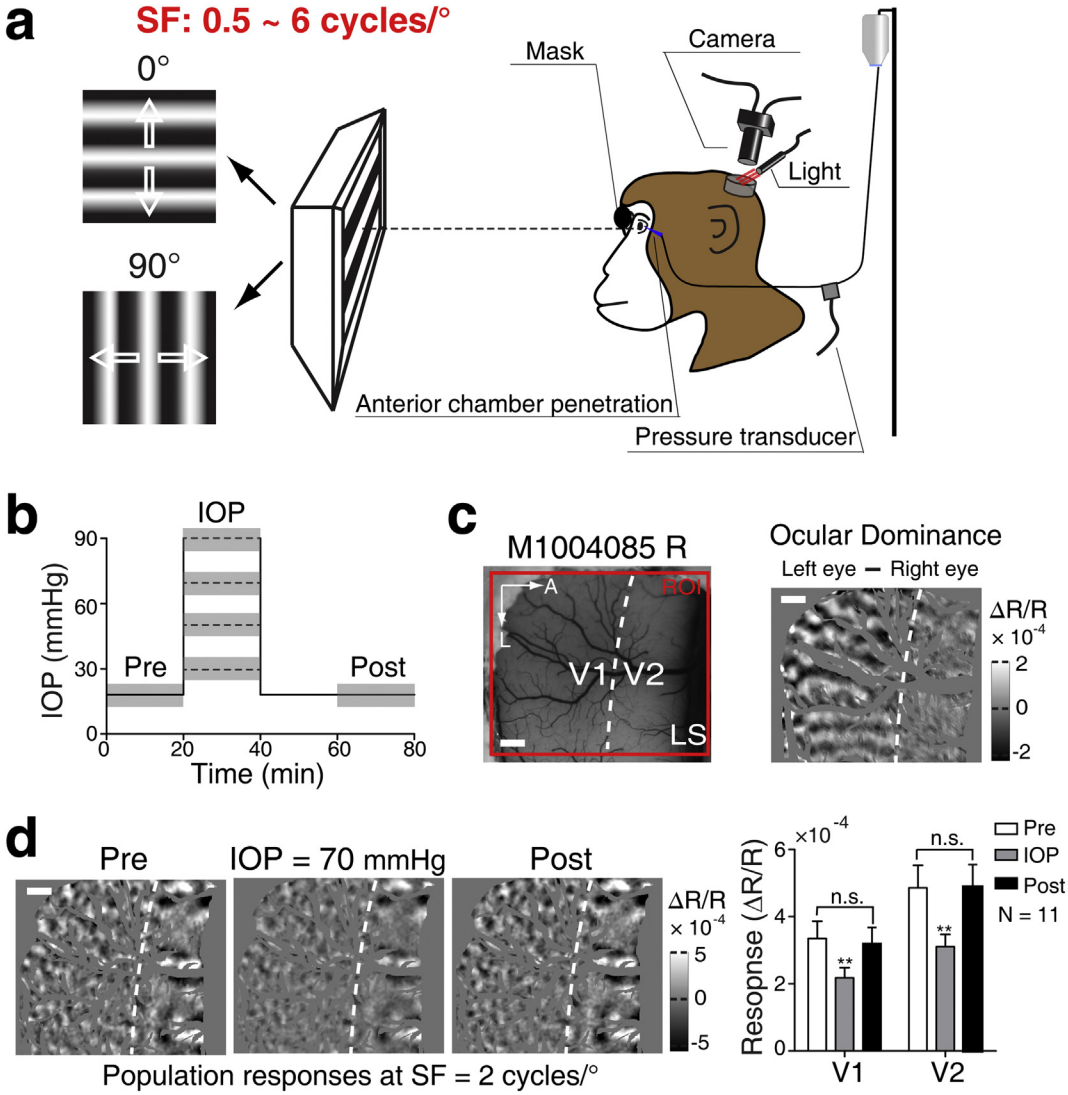

Fig. 1. Experimental protocol. (a) Schematic diagram of the experimental setup. 0° and 90° oriented sinusoidal gratings with a range of spatial frequencies (SFs) from 0.5 to 6 cycles/°, drifting at a fixed temporal frequency (5 Hz), were used to generate differential population responses. (b) The timeline of IOP elevation in each experiment. The dotted lines indicate various IOP levels (30, 50, 70, and 90 mmHg) for experiments. The gray rectangles indicate the periods of optical imaging recordings. Pre: before IOP elevation; IOP: IOP elevation; Post: after IOP elevation. (c) The region of interest (ROI) and the definition of V1 and V2 border. The left panel shows the cortical vasculature of simultaneously recorded V1 and V2, in monkey (M1004085) right hemisphere under 550 nm illumination. ROI for optical imaging is displayed by the red box. The white dotted line delimits the border of V1 and V2, defined according to the differential ocular dominance map (right panel) by subtracting responses to the left and right eyes. Note that ocular dominance domains exist in V1 and are absent in V2. LS, lunate sulcus; A, anterior; L, lateral. Scale bar, 1 mm. (d) The impact of IOP elevation on V1 and V2 responses. The differential orientation maps illustrate the changes of cortical population responses at SF = 2 cycles/° before, during and after IOP elevated to 70 mmHg, respectively. The specific values of cortical responses in V1 and V2 are shown in the right panel. Note that in experiments where IOP was elevated to 70 mmHg, the population response was observed to fully recover after the restoration normal of IOP in all our experiments. $N = 11$ hemispheres. n.s. represents $P > .05$. $^{**}P < .01$ compared with pre or post. Error bar denotes SEM.

stimuli SF in all seven monkeys. A previous investigation in cats reported that after the cancellation of the 20 min' IOP elevation at 90 mmHg, the electrophysiological functions of the retinal ganglion cells were gradually restored to the level before IOP elevation [17]. The duration of IOP elevation each time was approximately 18–20 min. In our first monkey experiment, we found that when IOP was elevated to 70 mmHg for 20 min, the population responses to oriented grating stimuli could fully recover in both V1 and V2 (Fig. 1d). By contrast, when IOP was elevated to 90 mmHg for 20 min, the cortical responses were only restored partially. During the transient IOP elevation, the optical media and fundus of the eye were routinely examined using ophthalmoscope. Neither corneal edema nor cataract was observed in our experimental setup, and optic nerve head as well as the optical refraction of the eye was not changed before, during and after IOP elevation.

2.3. Visual stimuli

A gamma-corrected CRT monitor (Sony G520, 21 in., 1280 × 960 pixels, 100 Hz, covering 40° × 30° visual angle) was placed 57 cm in front of the animal's eyes. The fovea of the experimental eye was back projected to the screen center using a reversing ophthalmoscope [18]. Visual stimuli were generated by custom-written software using MATLAB and Psychtoolbox-3. In all experiments, visual stimuli were presented monocularly (to the experimental eye) and the other eye was masked by the baffle plate. We used sinusoidal grating stimuli of orientation 0° and 90° to activate the cortical population responses (Fig. 1a). The SFs selected (0.5, 1, 2, 4, and 6 cycles/°) in our experiments were based on earlier electrophysiological single-unit recordings of parafovea areas of macaque V1 and V2 [19,20]. In these studies, the optimal SFs were about 3 cycles/° for V1 and about 1 cycle/° for V2.

Therefore, we used 2 cycles/° to maximally elicit cortical population responses in both V1 and V2 for our simultaneous recordings, consistent with our own previous optical imaging study [15]. Temporal frequency was 5 Hz in all experiments. All stimuli were presented at 100% contrast. The gratings moved back and forth perpendicularly to their orientations for 4 s (2 s for each direction). Retinal eccentricity maps were obtained with a horizontal or vertical light bar (width of 0.5°) moving upward or downward, or moving leftward or rightward at a speed of 2.33°/s on a dark background (covering 28° × 28° visual angle) [14,15].

2.4. Intrinsic-signal optical imaging and data analysis

All the procedures applied in our intrinsic-signal optical imaging system have been described earlier [14–16,21,22]. In brief, we used two Dalsa Pantera 1 M60 CCD cameras combined with two telecentric 55 mm f2.8 video lenses for simultaneously recording from regions of interest (ROI) in both V1 and V2 (Fig. 1c) in two chambers, one on each side of the skull. Within each trial, there were two conditions, including a pair of complementary visual stimuli (0° and 90° orientation pair). Under 630 ± 10 nm red light illumination, visual responses were recorded at 16 frames per second for a period of 8 s, including 1 s before stimulus onset. The inter-stimulus interval was 13 s.

During each phase of testing, i.e. during acute IOP elevation and equal periods of normal IOP (before and after IOP elevation), the orientation maps were averaged for 32 trials for stimuli of sine-wine gratings (32 repetitions at 0° and 90° stimulation respectively, for a total of approximately 18–20 min).Following IOP elevation, IOP was restored to normal and a period of 20 min allowed for retinal ganglion cell recovery from the effect of transient elevated IOP, during which we did not perform optical imaging. After recovery, the orientation map was again recorded under normal IOP (Fig. 1b).

For each stimulus condition, a single-condition map was constructed and the percent change of the light reflectance signal was calculated as follows: $\Delta R/R = (F_{avg} - F_0)/F_0$, in which $\Delta R/R$ is the percent change, F_0 represents a blank frame (the average response for the 1 s before stimulus onset), and F_{avg} is the average response over a 4 s epoch from 2 to 6 s after stimulus onset. Differential orientation maps were obtained by subtraction of a pair of single-condition maps activated by stimuli of orthogonal orientations (0° – 90°). A vector summation algorithm was applied to create orientation preference maps [23,24]. Blood vessels and other noisy areas were covered by a gray mask. Then the differential maps were highpass filtered (diameter: 1.1–1.2 mm) and smoothed (diameter: 106–306 μm) by circular averaging filters to suppress low- and high-frequency noise. In a differential orientation map, the average absolute values of $\Delta R/R$ in the responsive patches that preferred two stimulus conditions were treated as the cortical response. We took the cortical response before IOP elevation as the control, and then calculated the response ratio (IOP/control, %) during IOP elevation as an index to evaluate the IOP effects. Response profile analysis was performed to extract the orientation specificity encoded in the orientation maps [25,26]. Response profiles at different IOP levels were then normalized based on the control response and the changes of response magnitudes corresponding to each level of IOP elevation were evaluated. The boundary of V1 and V2 was defined classically using the ocular dominance mapping [27,28], which produced stripe-like compartments perpendicular to the border between V1 and V2 (Fig. 1c). The procedure for obtaining a retinal eccentricity map was described in previous studies [15,29,30]. In brief, a Fourier transform was first performed upon the image intensities obtained by moving-bar stimuli. Two phase maps acquired by stimuli of light bars moving in opposite directions were subtracted to remove the hemodynamic delay. The phase maps for horizontal and vertical bar stimuli were respectively converted to maps of elevation and azimuth, that in turn generated the final retinal eccentricity map.

2.5. Statistical analysis

One hemisphere of a monkey was excluded due to the leakage of silicone oil in the recording chamber. Therefore, 11 hemispheres from six monkeys were finally analyzed for the cortical responses to different IOP levels, and 13 hemispheres from seven monkeys for the cortical responses to various SFs under 70 mmHg. SPSS version 20.0 (SPSS, Inc., Chicago, IL, USA) was used for statistical analysis. All data are shown graphically as mean ± standard error of the mean (SEM). Two-tailed paired *t*-tests were performed to compare the cortical responses between individual IOP elevation and the control, and to compare the cortical response ratios during IOP elevation between V1 and V2 as well as between different retinal eccentricities. Spearman rank correlation was used to analyze the relationship between the cortical response ratios and the IOP levels, between the cortical response ratios and the SFs as well as between the cortical response ratios and the retinal eccentricities. A P value <.05 was considered statistically significant.

3. Results

To quantify the impact of acute IOP elevation on visual acuity, we performed precise modulation of acute IOP elevations in seven rhesus macaques. Due to ethical considerations, the perceptual visual acuity of monkeys cannot be simultaneously assessed in awake subjects during acute IOP elevation. Given that visual acuity depends on the transmission of fine spatial frequency (SF) information in the visual system, we directly examined the cortical SF responses using intrinsic-signal optical imaging in monkeys under generous anesthesia. The basics of our procedures for intrinsic-signal optical imaging are schematized in Fig. 1. Craniotomies were performed to expose V1 and V2, whose border was subsequently identified by ocular dominance mapping (Fig. 1c) followed by orientation mapping in both areas. Our assay of cortical response was the differential signal obtained in response to horizontal (0°) and vertical (90°) gratings. This was then measured under conditions of acute elevation of IOP (Fig. 1b). Neither corneal edema nor cataract was observed during transient IOP elevation in our experimental setup, and the optical refraction of the eye during IOP manipulation was not changed, through ophthalmoscope examinations. We found that IOP could be raised as high as 70 mmHg without preventing full recovery of population responses in both V1 and V2 upon restoration of normal of IOP (Fig. 1d).

3.1. Higher acute IOP elevations effect progressively greater decrements in cortical responses

To examine the impact of different IOP levels on the cortical responses to our stimuli, we fixed the SF of the oriented gratings at 2 cycles/°, which was the SF for eliciting robust intrinsic-signal population responses across V1 and V2 in our previous studies [14,15] (Fig. 1d and 2). A range of IOP elevations (30, 50, 70, and 90 mmHg) were performed in six monkeys. An example hemisphere shows that the monocular cortical response elicited in V1 and V2 decreased at higher IOP elevations in both areas, without changing the orientation preference maps (the colored maps) (Figs. 2a-2c). The cortical responses were calculated as the pixel intensity of the white and black patches. In order to illustrate the impact at different levels of IOP elevation, Fig. 2d shows orientation response profiles (i.e. the relative response within the differential orientation map amongst twelve compartments of equal area, subdivided by preferred orientation) [26]. Note that, as expected, the maximum responses occur in zones tuned to 0° or 90° in both V1 and V2 across all IOP elevations tested. Averaging across 11 out of 12 hemispheres, all IOP elevations from 30 to 90 mmHg significantly decreased cortical population responses in both V1 and V2 when compared with their controls (V1: 30 mmHg: $P = .043$, 50 mmHg: $P = .009$, 70 mmHg: $P = .001$, 90 mmHg: $P = .001$; V2: 30 mmHg: $P = .004$, 50 mmHg: $P = .002$, 70 mmHg: $P = .001$, 90 mmHg: $P < .001$; Fig. 2e). Note that one

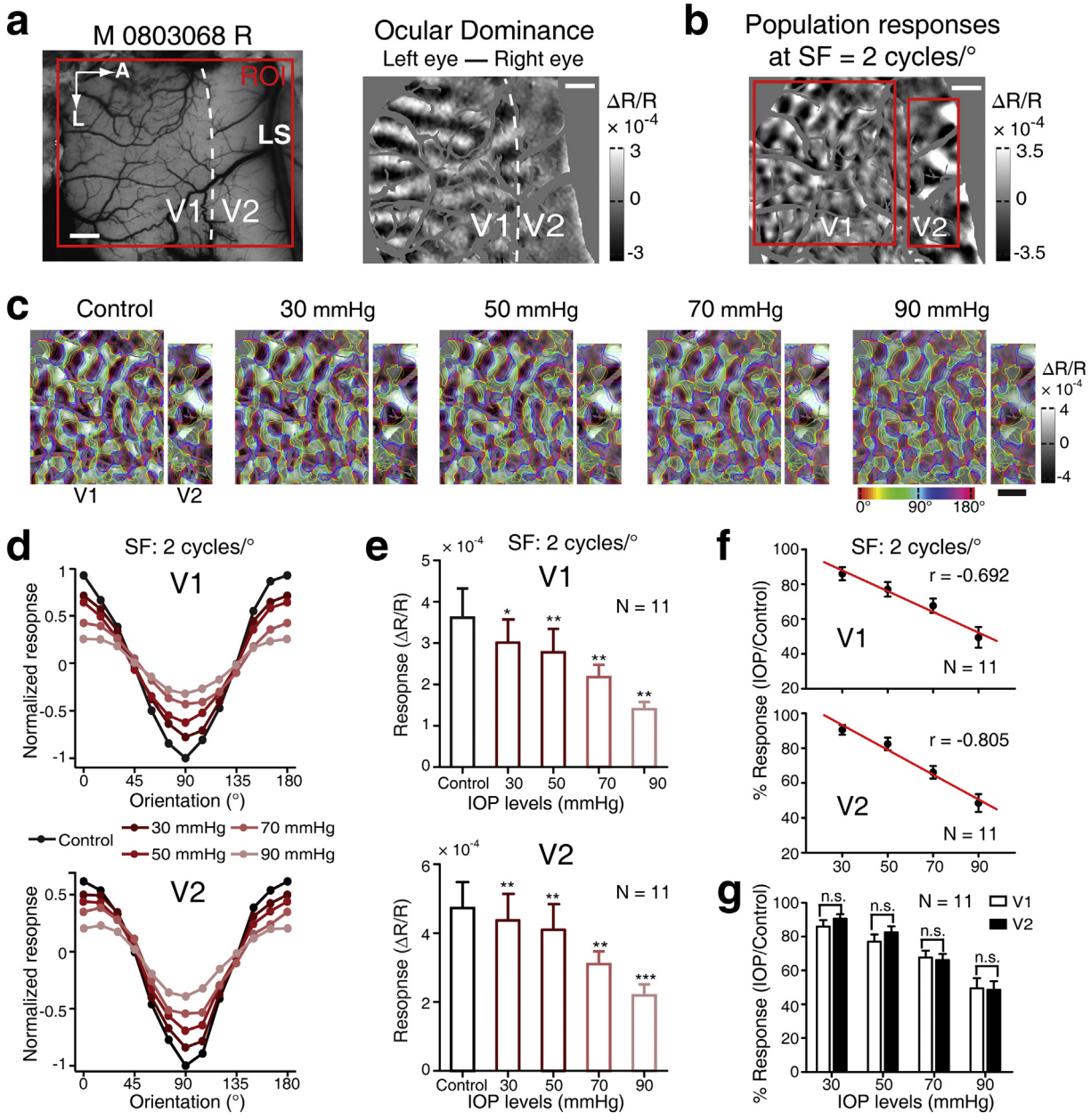

Fig. 2. Cortical responses in V1 and V2 during different levels of acute IOP elevation. (a) The left panel shows the cortical surface of V1 and V2 in the right hemisphere of exemplar monkey M0803068 and the ROI (red box) used for optical imaging. The white dotted line indicates the border of V1 and V2 obtained by the ocular dominance map shown in the right panel. LS, lunate sulcus; A, anterior; L, lateral. Scale bar, 1 mm. (b) The differential orientation population responses (0° − 90°) were obtained at SF = 2 cycles/°. The red boxes show the ROIs for V1 and V2. (c) Comparison of the population responses across different levels of IOP elevation (30, 50, 70, and 90 mmHg). Colored isoorientation contours were derived from orientation preference maps and were superimposed onto the gray differential orientation maps. The cortical responses before each IOP elevation were taken as controls. The control shown in the left is for IOP elevation of 30 mmHg. (d) Normalized response profile analysis derived from the population responses in (c). (e) Comparison of the cortical response (ΔR/R) during each IOP elevation with their controls. The control shown is for the period prior to 30 mmHg. $^{***}P < .001$, $^{**}P < .01$, $^{*}P < .05$. N = 11 hemispheres. (f) The negative relationship between the cortical response ratios (IOP/control, %). (g) The IOP levels in V1 and V2. N = 11 hemispheres. n.s. represents $P > .05$. Error bar denotes SEM.

hemisphere of a monkey was excluded due to technical reasons (see Methods). This result is also reflected in the plot of cortical response ratio (IOP elevation / control), indicating that the higher the IOP elevation, the more the decrease of the cortical responses (V1: $r = -0.692$, $P < .001$; V2: $r = -0.805$, $P < .001$; Fig. 2f). Finally, there was no statistical difference between V1 and V2 (Fig. 2g).

3.2. Cortical responses to higher SFs are more impaired during acute IOP elevation

70 mmHg is close to the IOP that is observed during the acute attack phase of primary angle-closure glaucoma in humans [6]. The cortical population responses at varied SFs across 13 hemispheres were thus investigated under 70 mmHg IOP in all seven monkeys. Fig. 3a and b present an example hemisphere showing differential orientation maps elicited with SFs ranging from 0.5 to 6 cycles/° in V1 and V2 before and during IOP elevation. The cortical responses seemed to become weaker during the IOP elevation when compared with the controls, and this was more evident at high SF toward 6 cycles/° (Fig. 3a and b). We then calculated the average response amplitude across all 13 hemispheres and found that the cortical responses in both V1 and V2 were in fact significantly decreased at 70 mmHg across all SFs tested (V1: $P <$ .001 for SFs = 0.5, 1, 2 and 6 cycles/° and $P = .013$ for SF = 4 cycles/°; V2: $P < .001$ for SFs = 0.5, 1, 2 and 4 cycles/° and $P = .002$ for SF = 6

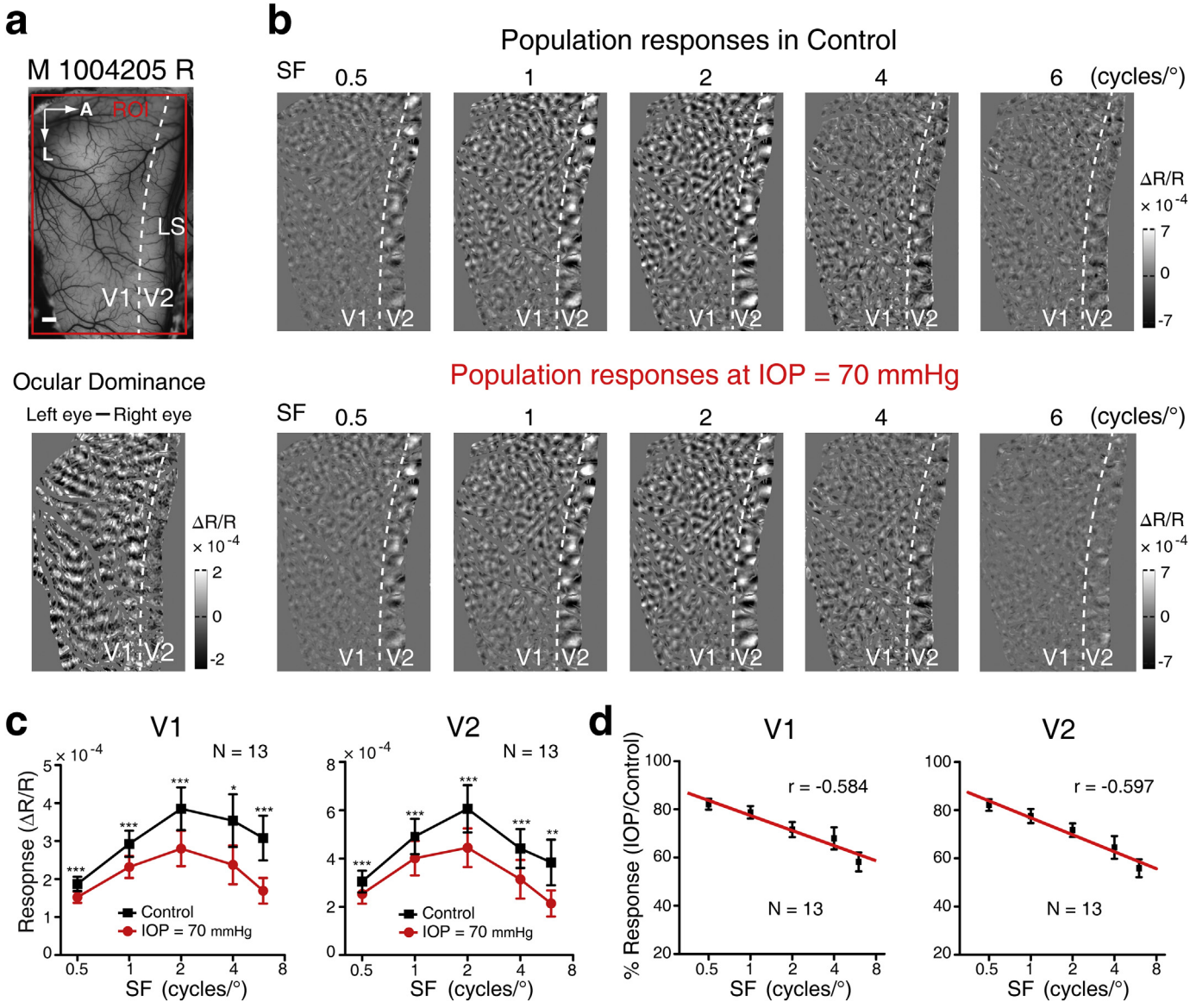

Fig. 3. The impact of acute IOP elevation on the cortical responses at varied SFs. (a) Cortical vasculature of V1 and V2 in monkey (M1004205) right hemisphere (Upper), and definition of the border of V1 and V2 (Lower). LS, lunate sulcus; A, anterior; L, lateral. Scale bar, 1 mm. (b) Differential orientation maps (0° — 90°) obtained at five different SFs (specified above each map) before (control) and during IOP elevation to 70 mmHg. (c) Statistics of the cortical population responses elicited at different SFs in V1 and V2 before and during IOP elevation across 13 hemispheres. $^{***}P < .001$, $^{**}P < .01$, $^{*}P < .05$. (d) The relationship between the cortical response ratios (IOP/control, %) and the stimulus SFs. $N = 13$ hemispheres. Error bar denotes SEM.

cycles/°; Fig. 3c). The magnitude of the reduction of cortical responses between control and IOP elevation was progressively larger for higher SFs (Fig. 3d). This apparent trend was corroborated by Spearman correlation analysis, showing that the cortical response ratio (IOP elevation / control) decreased significantly as the SF increased, in both V1 and V2 (V1: $r = -0.584$, $P < .001$; V2: $r = -0.597$, $P < .001$) (Fig. 3d). These results reveal that sharp IOP elevation significantly reduces cortical responses across the full range of SFs tested, as might result from combined impairment of both the magnocellular and parvocellular channels. A more secure inference, as high SFs were more severely affected, is that parvocellular function may be relatively more susceptible than magnocellular function to sharp IOP elevation.

3.3. Cortical responses at smaller retinal eccentricities are more affected during acute IOP elevation

Visual acuity peaks at the fovea and declines steeply with eccentricity (the distance from the fovea) [31]. We thus examined the impact of sharp IOP elevation on cortical responses at different retinal eccentricities. We performed this analysis for area V1 of nine hemispheres with larger ROIs that spanned approximately 4–9° eccentricity. Fig. 4a presents a retinal eccentricity map of V1 in an example hemisphere, together with cortical population responses bounded by isoeccentricity contours. We firstly studied the population responses in V1 at a finer scale, a 0.5° interval within the 4–9° eccentricity maps across all nine hemispheres tested. Spearman correlation analysis showed that the cortical responses decreased in a linear fashion with diminishing eccentricity during 70 mmHg IOP; this finding was reliably replicated at each SF tested (0.5 cycle/°: $r = 0.691$, $P < .001$; 1 cycle/°: $r = 0.544$, $P < .001$; 2 cycles/°: $r = 0.536$, $P < .001$; 4 cycles/°: $r = 0.436$, $P < .001$; 6 cycles/°: $r = 0.420$, $P < .001$) (Fig. 4b). We then divided the ROI into two regions with larger and smaller eccentricity (6–9° vs. 4–6°) and found, at every SF tested, that the cortical responses were more depressed in the region of smaller eccentricity than those in the region with larger eccentricity when IOP was elevated sharply to 70 mmHg (0.5 cycle/°: $P = .009$; 1 cycle/°: $P = .008$; 2 cycles/°: $P = .005$; 4 cycles/°: $P = .032$; 6 cycles/°: $P = .004$) (Fig. 4c). These results reveal that V1 responses at smaller eccentricity are more impaired than

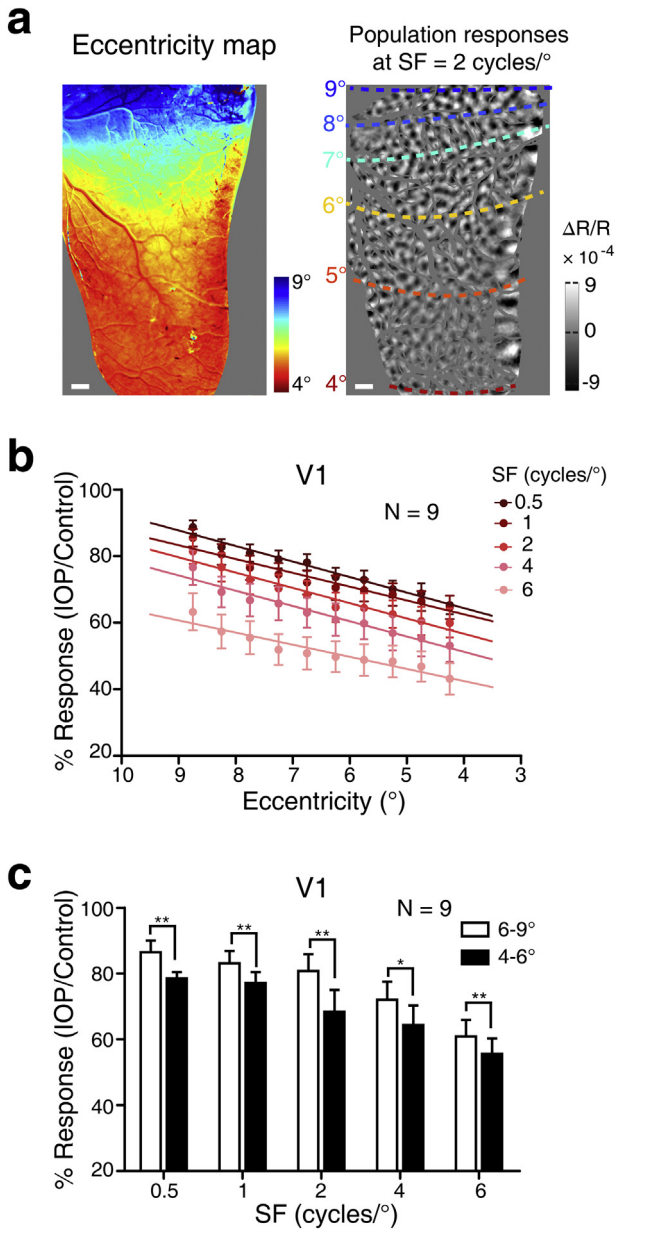

Fig. 4. Cortical responses at different retinal eccentricities during acute IOP elevation. (a) The left panel shows an example retinal eccentricity map of the cortical surface in V1 and V2. The corresponding cortical vasculature map is displayed in Fig. 3A. Cortical population responses at an SF of 2 cycles/° with superimposed isoeccentricity contours are shown in the right panel. Scale bar, 1 mm. (b) Parametric relationship between the cortical response ratios and eccentricity for each SF during 70 mmHg IOP. (c) Statistics of the cortical response ratios (70 mmHg IOP: control) between larger eccentricity (6–9°) and smaller eccentricity (4–6°) zones in V1, at each SF tested. $^{**}P < .01$, $^{*}P < .05$. N = nine hemispheres. Error bar denotes SEM.

those at larger eccentricity, indicating – if this trend were to be maintained further toward the fovea – that sharp IOP elevation is relatively more deleterious for high acuity vision.

4. Discussion

Previous clinical works have attempted to identify the causes of visual acuity loss following acute primary angle-closure glaucoma. Accompanying the attack of sharp IOP elevation, pathologies of the affected eye such as cataract and corneal edema along with surgical interventions are the common complications [7]. These optical complications prevent the establishment of the exact relationship between acute IOP elevation and visual acuity. How visual acuity is affected by acute IOP changes has therefore remained unclear.

To date, physiological assessment of the consequences of sharp IOP elevation upon visual responses in primate cortex has been lacking, particularly its impact on the basis of visual acuity in a condition analogous to the acute attack phase of primary angle-closure glaucoma in humans. In the present study, we used intrinsic-signal optical imaging to investigate changes of the cortical population responses to oriented grating stimuli at varied SFs during acute IOP elevation in macaque monkeys. First, we examined the impact of different acute IOP elevations on the cortical population responses simultaneously recorded over large visual areas of V1 and V2. As expected, we found that the cortical responses decreased as the IOP increased, with a similar magnitude of response decrement across V1 and V2 (Figs. 1 and 2). Next, we sharply elevated IOP to 70 mmHg and examined the impact on cortical responses at various SFs and at different eccentricities. The consequences of this sharp IOP elevation are summarized by two principal findings: (i) that it preferentially depresses higher-SF cortical responses across all eccentricities within the parafoveal range examined (Fig. 3), and (ii) preferentially depresses responses at more central eccentricities across a range of tested SFs (Fig. 4). These results show that impairment of fine visual discrimination within the central visual field is the principal consequence of sharp IOP elevation in macaque monkeys.

The primate retina is populated by many subtypes of output cell, amongst which the most prominent are parasol and midget ganglion cells, distinguished by multiple morphological and physiological characteristics [32]. Parasol ganglion cells (that project to the magnocellular layers of the lateral geniculate nucleus [LGN]), have larger cell bodies, more extensive dendritic arborisation and, in consequence, larger receptive fields. Midget ganglion cells (that project to the parvocelluar layers of the LGN), are by far the more numerous, especially in central retina, but their proportion in relation to all ganglion cells declines with eccentricity, whilst that of parasol cells rises [32–34]. Magnocellular and parvocellular layers in the LGN then connect to 4Cα and 4Cβ layers in V1 respectively [35]. After that, the magnocellular and parvocellular channels converge relatively homogenously within the superficial layers of V1 [36,37], and V2 in turn inherits integrated magnocellular/parvocellular signals [38]. The finer sampling of visual space by the parvocellular channel affords it better spatial acuity, as evidenced by the severe loss of behavioural acuity produced by experimental parvocellular lesions in task-trained macaques, and the absence of such loss with magnocellular lesions [13,39]. At the physiological level, the two parallel pathways have distinct SF preferences: the magnocellular pathway prefers lower SF (and higher TF) and processes a fast "coarse" sweep of the visual information, while the parvocellular pathway prefers higher SF and provides "fine" discrimination of objects [35,40].

Our findings suggest that acutely raising IOP by 70 mmHg has more deleterious consequences for the parvocellular compared to the magnocellular system. The inference relies upon previous selective lesion studies [41,42] that have determined the spatio-temporal contrast sensitivity of each system operating in isolation: firstly, that both systems should be jointly activated under our stimulus conditions (5 Hz, high contrast) and co-drive cortical responses across the full range of SFs tested; secondly that the parvocellular system should contribute a greater proportion of drive as it gains in relative sensitivity toward higher SFs. Hence the observed, systematic reduction of cortical response toward higher SFs, in both V1 and V2, indicates that the parvocellular system is the more severely impaired. A similar chain of reasoning applies to our second principal finding, that acute IOP elevation effected a progressively greater reduction of cortical response at more central retinotopic loci of V1 (with small eccentricities). This held for all SFs tested, and the regression data (Fig. 4b) is very orderly. By further comparing the effects on cortical responses between smaller (4° – 6°) and larger (6° – 9°) eccentricities, we showed that high IOP elevation had less effect at larger eccentricities across all SFs tested

(Fig. 4c). This pattern may result from the fact that, as mentioned above, the local ratio of midget:parasol cells increases toward the fovea [32–34]. The relative numbers of units in the LGN follow suit, meaning that the proportion of cortical drive attributable to the parvocellular system is correspondingly heavier toward central field. If all that holds, it allows us to infer once again that IOP elevation is more harmful to parvocellular function than to magnocellular function. Further experiments using stimuli that aim to more selectively "isolate" the two pathways could validate this inference.

Unlike chronic glaucoma, where evidence from clinical and psychophysical assessment of human subjects converges with anatomical studies of animal models to suggest early vulnerability of the magnocellular system [43–45], with longer term retinal ganglion cell loss that may be more indiscriminate [45–48], a limited body of work on acute IOP elevation points toward a more specific pathology. Pioneering electrophysiological studies in the cat by Shou et al. [49] and Zhou et al. [17] showed that acute IOP elevation caused preferential loss of responsivity by X cells (likely homologous to midget cells in primates) in the retina and LGN. The suggested mechanism was greater vulnerability of X ganglion cells to retinal ischemia. Chen et al. [50] later revealed that the cortical population responses in cats were affected more severely when high-SF gratings (1.2 cycles/°) were used during brief increased IOP (4 min at 80 mmHg), again indicating that the X pathway was more vulnerable. Dandona et al. [51], examining the efficacy of axonal transport to the LGN of macaque monkeys, reported that in one out of four subjects tested with 12-h acute, severe IOP elevation, transport was reduced more to parvocellular than to magnocellular layers. Although this study was inconclusive, it suggests that acute IOP elevation can lead to the death of retinal ganglion cells, causing the selective atrophy of the midget retinal projection to LGN.

Previous research using chronic high-IOP monkey models and studies of chronic glaucoma patients have suggested that magnocellular cells are affected earlier than parvocellular cells in the retina and LGN [43–45,51–55]. Thus, it is proposed that magnocellular cells suffer selective loss at the early stage of chronic glaucoma. As is well known, "optic disk cupping" is a typical characteristics of chronic glaucoma, in which the superior and inferior portions of the optic disk have less connective tissue and hence are more vulnerable than the nasal and temporal portions [56]. Moreover, the superior and inferior portions of the optic disk receive nerve fibers from ganglion cells in the mid-peripheral retina and carry a higher proportion of magnocellular signals [32,57]. Therefore, the hypothesis that magnocellular cells are sensitive to chronic IOP elevation is based upon the injured regions of the optic disk. In addition, it has been proposed that magnocellular cells may be inherently intolerant to the chronic increased IOP [54]. However, the patterns of optic disk damage differ between acute and chronic glaucoma [1,6]. For an acute attack of primary angle-closure glaucoma, if not treated in time, the optic disk can present as "pale" caused by extremely high IOP instead of "cupping" [6]. This suggests that optic nerve injury is governed by different mechanisms in acute and chronic IOP elevation. In the present study, the transient IOP elevation did not cause irreversible damage to the ganglion cells, but might initiate the early phase of the functional impairment of ganglion cells. The neural mechanisms underlying apoptosis and atrophy of retinal ganglion cells resulting from acute high IOP needs further exploration in future studies.

In summary, our findings provide direct neural evidence of the impact of acute IOP elevation on visual acuity in non-human primates. We show that fine visual acuity is immediately impaired during acute sharp IOP elevation, in contrast to the early stage of chronic glaucoma where fine visual acuity is relatively invulnerable. Our study provides first-hand evidences for ophthalmologists that acute glaucoma should be treated in a timely fashion in order to preserve fine visual acuity.

Funding sources

This research was supported by the Shanghai Municipal Science and Technology Major Project (No. 2018SHZDZX05 to W. Wang), the National Natural Science Foundation of China (No. 81430007 to X.H. Sun, No. 81790641 to X.H. Sun, and No.31600846 to N.N. Yuan), the Strategic Priority Research Program of Chinese Academy of Sciences (No. XDB32060200 to W. Wang), the Shanghai Committee of Science and Technology (No.17410712500 to X.H. Sun) and the top priority of clinical medicine center of Shanghai (No.2017ZZ01020 to X.H. Sun). The sponsor or funding organization had no role in the design or conduct of this research.

Competing interests

The authors declare no competing interests.

References

[1] Jonas JB, Aung T, Bourne RR, Bron AM, Ritch R, Panda-Jonas S. Glaucoma. Lancet 2017;390(10108):2183–93.
[2] Prum Jr BE, Herndon Jr LW, Moroi SE, Mansberger SL, Stein JD, Lim MC, et al. Primary angle closure preferred practice pattern((R)) guidelines. Ophthalmology 2016;123(1):P1–P40.
[3] Prum Jr BE, Lim MC, Mansberger SL, Stein JD, Moroi SE, Gedde SJ, et al. Primary open-angle glaucoma suspect preferred practice pattern((R)) guidelines. Ophthalmology 2016;123(1):P112–51.
[4] Li MW, Chen YH, Chen XX, Zhu WQ, Chen XL, Wang XL, et al. Differences between fellow eyes of acute and chronic primary angle closure (glaucoma): An ultrasound biomicroscopy quantitative study. PLoS One 2018;13(2).
[5] Li MW, Chen YH, Jiang ZY, Chen XX, Chen JY, Sun XH. What are the characteristics of primary angle closure with longer axial length? Invest Ophthalmol Vis Sci 2018;59(3):1354–9.
[6] Sun X, Dai Y, Chen Y, Yu DY, Cringle SJ, Chen J, et al. Primary angle closure glaucoma: what we know and what we don't know. Prog Retin Eye Res 2017;57:26–45.
[7] Andreatta W, Nessim M, Nightingale P, Shah P. ReGAE 10: long-term visual acuity outcomes after acute primary angle closure. J Glaucoma 2014;23(4):206–10.
[8] Cavonius CR, Robbins DO. Relationships between luminance and visual-acuity in rhesus-monkey. J Physiol-London 1973;232(2):239–46.
[9] Weinstein B, Grether WF. A comparison of visual acuity in the rhesus monkey and man. J Comp Psychol 1940;30(2):187–95.
[10] Merigan WH, Barkdoll E, Maurissen JPJ, Eskin TA, Lapham LW. Acrylamide effects on the macaque visual-system 1 psychophysics and electrophysiology. Invest Ophthalmol Vis Sci 1985;26(3):309–16.
[11] Tootell RBH, Silverman MS, Hamilton SL, Switkes E, Devalois RL. Functional-anatomy of macaque striate cortex. 5. Spatial-frequency. J Neurosci 1988;8(5):1610–24.
[12] Merigan WH, Maunsell JHR. How parallel are the primate visual pathways. Annu Rev Neurosci 1993;16:369–402.
[13] Schiller PH, Logothetis NK. The color-opponent and broad-band channels of the primate visual-system. Trends Neurosci 1990;13(10):392–8.
[14] An X, Gong HL, Qian LL, Wang XC, Pan YX, Zhang X, et al. Distinct functional organizations for processing different motion signals in V1, V2, and V4 of macaque. J Neurosci 2012;32(39):13363–79.
[15] Lu Y, Yin J, Chen Z, Gong H, Liu Y, Qian L, et al. Revealing detail along the visual hierarchy: neural clustering preserves acuity from V1 to V4. Neuron 2018;98(2):417–28 e3.
[16] Pan Y, Chen M, Yin J, An X, Zhang X, Lu Y, et al. Equivalent representation of real and illusory contours in macaque V4. J Neurosci 2012;32(20):6760–70.
[17] Zhou Y, Wang W, Ren B, Shou T. Receptive field properties of cat retinal ganglion cells during short-term IOP elevation. Invest Ophthalmol Vis Sci 1994;35(6):2758–64.
[18] Jones HE, Grieve KL, Wang W, Sillito AM. Surround suppression in primate V1. J Neurophysiol 2001;86(4):2011–28.
[19] Foster KH, Gaska JP, Nagler M, Pollen DA. Spatial and temporal frequency selectivity of neurones in visual cortical areas V1 and V2 of the macaque monkey. J Physiol 1985;365:331–63.
[20] Levitt JB, Kiper DC, Movshon JA. Receptive fields and functional architecture of macaque V2. J Neurophysiol 1994;71(6):2517–42.
[21] An X, Gong HL, McLoughlin N, Yang YP, Wang W. The mechanism for processing random-dot motion at various speeds in early visual cortices. PLoS One 2014;9(3).
[22] Schiessl I, Wang W, McLoughlin N. Independent components of the haemodynamic response in intrinsic optical imaging. Neuroimage 2008;39(2):634–46.
[23] Ribot J, Tanaka S, Tanaka H, Ajima A. Online analysis method for intrinsic signal optical imaging. J Neurosci Methods 2006;153(1):8–20.
[24] Blasdel GG, Salama G. Voltage-sensitive dyes reveal a modular organization in monkey striate cortex. Nature 1986;321(6070):579–85.
[25] Adesnik H, Bruns W, Taniguchi H, Huang ZJ, Scanziani M. A neural circuit for spatial summation in visual cortex. Nature 2012;490(7419):226–31.
[26] Basole A, White LE, Fitzpatrick D. Mapping multiple features in the population response of visual cortex. Nature 2003;423(6943):986–90.

[27] Blasdel GG. Differential imaging of ocular dominance and orientation selectivity in monkey striate cortex. J Neurosci 1992;12(8):3115–38.
[28] Ts'o DY, Frostig RD, Lieke EE, Grinvald A. Functional organization of primate visual cortex revealed by high resolution optical imaging. Science 1990;249(4967):417–20.
[29] Vanni MP, Provost J, Lesage F, Casanova C. Evaluation of receptive field size from higher harmonics in visuotopic mapping using continuous stimulation optical imaging. J Neurosci Methods 2010;189(1):138–50.
[30] Kalatsky VA, Stryker MP. New paradigm for optical imaging: temporally encoded maps of intrinsic signal. Neuron 2003;38(4):529–45.
[31] Merigan WH, Katz LM. Spatial-resolution across the macaque retina. Vis Res 1990;30(7):985–91.
[32] Dacey DM. Physiology, morphology and spatial densities of identified ganglion-cell types in primate retina. Ciba F Symp 1994;184:12–28.
[33] Azzopardi P, Jones KE, Cowey A. Uneven mapping of magnocellular and parvocellular projections from the lateral geniculate nucleus to the striate cortex in the macaque monkey. Vis Res 1999;39(13):2179–89.
[34] Silveira LCL, Perry VH. The topography of magnocellular projecting ganglion-cells (M-ganglion cells) in the primate retina. Neuroscience 1991;40(1):217–37.
[35] Nassi JJ, Callaway EM. Parallel processing strategies of the primate visual system. Nat Rev Neurosci 2009;10(5):360–72.
[36] Malpeli JG, Schiller PH, Colby CL. Response properties of single cells in monkey striate cortex during reversible inactivation of individual lateral geniculate laminae. J Neurophysiol 1981;46(5):1102–19.
[37] Nealey TA, Maunsell JH. Magnocellular and parvocellular contributions to the responses of neurons in macaque striate cortex. J Neurosci 1994;14(4):2069–79.
[38] Sincich LC, Horton JC. The circuitry of V1 and V2: integration of color, form, and motion. Annu Rev Neurosci 2005;28:303–26.
[39] Merigan WH, Katz LM, Maunsell JHR. The effects of Parvocellular lateral geniculate lesions on the acuity and contrast sensitivity of macaque monkeys. J Neurosci 1991;11(4):994–1001.
[40] Callaway EM. Structure and function of parallel pathways in the primate early visual system. J Physiol-Lond 2005;566(1):13–9.
[41] Merigan WH, Byrne CE, Maunsell JHR. Does primate motion perception depend on the magnocellular pathway. J Neurosci 1991;11(11):3422–9.
[42] Merigan WH, Eskin TA. Spatio-temporal vision of macaques with severe loss of P beta retinal ganglion cells. Vis Res 1986;26(11):1751–61.
[43] Quigley HA, Dunkelberger GR, Green WR. Retinal ganglion-cell atrophy correlated with automated Perimetry in human eyes with glaucoma. Am J Ophthalmol 1989;107(5):453–64.
[44] Quigley HA, Sanchez RM, Dunkelberger GR, L'Hernault NL, Baginski TA. Chronic glaucoma selectively damages large optic nerve fibers. Invest Ophthalmol Vis Sci 1987;28(6):913–20.
[45] Zhang P, Wen W, Sun X, He S. Selective reduction of fMRI responses to transient achromatic stimuli in the magnocellular layers of the LGN and the superficial layer of the SC of early glaucoma patients. Hum Brain Mapp 2016;37(2):558–69.
[46] Ansari EA, Morgan JE, Snowden RJ. Psychophysical characterisation of early functional loss in glaucoma and ocular hypertension. Brit J Ophthalmol 2002;86(10):1131–5.
[47] Crawford MLJ, Harwerth RS, Smith EL, Shen F, Carter-Dawson L. Glaucoma in primates: cytochrome oxidase reactivity in parvo- and magnocellular pathways. Invest Ophthalmol Vis Sci 2000;41(7):1791–802.
[48] Martin L, Wanger P, Vancea L, Gothlin B. Concordance of high-pass resolution perimetry and frequency-doubling technology perimetry results in glaucoma: no support for selective ganglion cell damage. J Glaucoma 2003;12(1):40–4.
[49] Shou TD, Zhou YF. Y-cells in the cat retina are more tolerant than X-cells to brief elevation of Iop. Invest Ophthalmol Vis Sci 1989;30(10):2093–8.
[50] Chen X, Sun C, Huang L, Shou T. Selective loss of orientation column maps in visual cortex during brief elevation of intraocular pressure. Invest Ophthalmol Vis Sci 2003;44(1):435–41.
[51] Dandona L, Hendrickson A, Quigley HA. Selective effects of experimental glaucoma on axonal-transport by retinal ganglion-cells to the dorsal lateral geniculate-nucleus. Invest Ophthalmol Vis Sci 1991;32(5):1593–9.
[52] Chaturvedi N, Hedleywhyte ET, Dreyer EB. Lateral geniculate-nucleus in glaucoma. Am J Ophthalmol 1993;116(2):182–8.
[53] Ito Y, Shimazawa M, Chen YN, Tsuruma K, Yamashima T, Araie M, et al. Morphological changes in the visual pathway induced by experimental glaucoma in Japanese monkeys. Exp Eye Res 2009;89(2):246–55.
[54] Quigley HA, Dunkelberger GR, Green WR. Chronic human glaucoma causing selectively greater loss of large optic nerve fibers. Ophthalmology 1988;95(3):357–63.
[55] Weber AJ, Chen H, Hubbard WC, Kaufman PL. Experimental glaucoma and cell size, density, and number in the primate lateral geniculate nucleus. Invest Ophthalmol Vis Sci 2000;41(6):1370–9.
[56] Hood DC. Improving our understanding, and detection, of glaucomatous damage: an approach based upon optical coherence tomography (OCT). Prog Retin Eye Res 2017;57:46–75.
[57] Silveira LCL, Saito CA, Lee BB, Kremers J, da Silva M, Kilavik BE, et al. Morphology and physiology of primate M- and P-cells. Prog Brain Res 2003;144:21–46.